



This is a repository copy of *Orthogonally polarised dual-channel directional modulation based on crossed-dipole arrays*.

White Rose Research Online URL for this paper:
<https://eprints.whiterose.ac.uk/143728/>

Version: Accepted Version

Article:

Zhang, B., Liu, W. orcid.org/0000-0003-2968-2888 and Lan., X. (2019) Orthogonally polarised dual-channel directional modulation based on crossed-dipole arrays. *IEEE Access*, 7. pp. 34198-34206. ISSN 2169-3536

<https://doi.org/10.1109/access.2019.2903909>

© 2019 IEEE. Personal use of this material is permitted. Permission from IEEE must be obtained for all other users, including reprinting/ republishing this material for advertising or promotional purposes, creating new collective works for resale or redistribution to servers or lists, or reuse of any copyrighted components of this work in other works. Reproduced in accordance with the publisher's self-archiving policy.

Reuse

Items deposited in White Rose Research Online are protected by copyright, with all rights reserved unless indicated otherwise. They may be downloaded and/or printed for private study, or other acts as permitted by national copyright laws. The publisher or other rights holders may allow further reproduction and re-use of the full text version. This is indicated by the licence information on the White Rose Research Online record for the item.

Takedown

If you consider content in White Rose Research Online to be in breach of UK law, please notify us by emailing eprints@whiterose.ac.uk including the URL of the record and the reason for the withdrawal request.



eprints@whiterose.ac.uk
<https://eprints.whiterose.ac.uk/>

Date of publication xxxx 00, 0000, date of current version xxxx 00, 0000.

Digital Object Identifier 10.1109/ACCESS.2017.DOI

Orthogonally Polarised Dual-Channel Directional Modulation Based on Crossed-Dipole Arrays

BO ZHANG¹, (MEMBER, IEEE), WEI LIU², (SENIOR MEMBER, IEEE), AND XIANG LAN.²

¹College of Electronic and Communication Engineering, Tianjin Normal University, Tianjin, 300387, China (e-mail: b.zhangintj@outlook.com)

²Communications Research Group, Department of Electronic and Electrical Engineering, University of Sheffield, Sheffield S1 4ET, United Kingdom (e-mail: w.liu@sheffield.ac.uk; xlan2@sheffield.ac.uk)

Corresponding authors: Bo Zhang (e-mail: b.zhangintj@outlook.com), Wei Liu (e-mail: w.liu@sheffield.ac.uk).

ABSTRACT Directional modulation (DM) as a physical layer security technique has been studied based on traditional antenna arrays; however, in most of the designs, only one signal is transmitted at one carrier frequency. In this paper, signal polarisation information is exploited, and a new DM scheme is designed which can transmit a pair of orthogonal polarised signals to the same direction at the same frequency simultaneously, resulting in doubled channel capacity. These two signals can also be considered as one composite signal using a four dimensional (4-D) modulation scheme across the two polarisation diversity channels. Moreover, compressive sensing (CS) based formulations for designing sparse crossed-dipole arrays in this context are proposed to exploit the degrees of freedom in the spatial domain for further improved performance, as demonstrated by various design examples.

INDEX TERMS Crossed-dipole array, directional modulation, orthogonal polarisation

I. INTRODUCTION

DIRECTIONAL modulation (DM) as a physical layer security technique was introduced in [1], [2] by keeping desired constellation points in an interested direction or directions, while scrambling them for the remaining directions. A procedure based on reconfigurable antenna arrays on how to switch elements for transmitting symbols un-distorted in a specified direction was described in [3]. Phased arrays were also applied to the DM design with a single carrier frequency [4], [5] and multi-carrier frequencies [6]. Multiple input multiple output (MIMO) and artificial-noise (AN)-aided designs [7]–[10] were used to achieve DM as well. In [11], a dual-beam DM scheme was proposed to synthesize a DM signal, where unlike the traditional transmitter, the in-phase and quadrature signals were excited by two antennas. In [12], a DM based two element antenna array was studied, followed by a pattern synthesis method in [13], an artificial-noise-aided zero-forcing synthesis approach in [14], and a multi-relay design in [15]. Static and dynamic interference were combined together and added into the DM design, then a more security performance based on the same level of transmission power can be achieved [16]. Recently, DM was extended to multi-path channel models [17], [18], which

helps improve security of the system when the eavesdroppers are very close to the desired position, and DM was also applied to sparse array design [18] to further exploit the degrees of freedom (DOFs) in the spatial domain.

However, in the current DM field, only one signal is transmitted at one carrier frequency to the desired direction. To increase channel capacity, in this paper we exploit the polarisation information of the electromagnetic signal, and two orthogonally polarised signals can be transmitted to the same direction at the same frequency simultaneously without crossover, as demonstrated in our recent conference publication [19]. These two signals can also be considered as one composite signal using the four dimensional (4-D) modulation scheme across the two polarisation diversity channels [20]–[22]. This can be achieved by employing polarisation-sensitive arrays, such as tripole arrays and crossed-dipole arrays [20], [23]–[30]. To receive and separate the two orthogonally polarised signals, a crossed-dipole antenna or array can be employed at the receiver side [30], and polarisations of the antennas at the receiver side do not need to match those of the transmitters, as cross-interference due to a mismatch or channel distortion can be suppressed using standard signal processing techniques, such as the Wiener

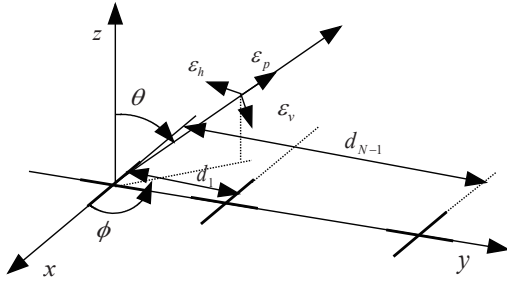


FIGURE 1: A linear crossed-dipole array.

filter when a reference signal is available [20].

Moreover, compared to [19], to reduce the number of antennas and further exploit the DOFs [31], [32] in the spatial domain, the orthogonally polarised design for DM is applied to sparse antenna arrays. In this work, similar to the design in [5], [6], we apply compressive sensing (CS) based formulation to the design. In the context of M-ary signaling for modulation, assume there are M symbols for each of the two signals s_1 and s_2 . Then, for the two signals transmitted simultaneously, there will be M^2 combined symbols in total. The key is to find a set of common crossed-dipole locations for all M^2 combined symbols, which can be solved using the group sparsity technique [33]; otherwise, we would have different antenna locations for different combined symbols.

Overall, the contribution of the work is two-fold: firstly, we exploit the polarisation information and extend the traditional DM design to the dual-polarised antenna arrays; secondly, a sparse array design method is proposed to reduce the number of dual-polarised antennas by exploiting the DOFs in the spatial domain.

The remaining part is organised as follows. A review of crossed-dipole arrays is given in Sec. II. DM design for a pair of orthogonally polarised signals transmitted from a given array geometry and an array with optimised crossed-dipole locations are considered in Sec. III. Design examples are presented in Sec. IV and conclusions drawn in Sec. V.

II. POLARISATION-SENSITIVE BEAMFORMING BASED ON CROSSED-DIPOLE ARRAYS

Fig. 1 shows the structure of an N-element linear crossed-dipole array. Each antenna has two orthogonally orientated dipoles, one parallel to the x-axis with a complex-valued coefficient $w_{n,x}$, and one parallel to the y-axis with coefficient $w_{n,y}$, $n = 0, \dots, N - 1$. The zeroth antenna located at the transmitter coordinate origin is assumed as the reference point. The spacing between the zeroth and the n-th antenna is denoted by d_n ($n = 1, \dots, N - 1$), and the aperture of the array is d_{N-1} . The elevation angle and azimuth angle are denoted by $\theta \in [0, \pi]$ and $\phi \in [0, 2\pi]$, respectively.

For a transverse electromagnetic (TEM) wave in the far-field from the transmitter array, ε_p is considered as the unit vector of the transmission direction of the TEM wave, and ε_h and ε_v are two orthogonal unit vectors and also at right angle

to ε_p , i.e., $\varepsilon_h \cdot \varepsilon_v = 0$, $\varepsilon_h \cdot \varepsilon_p = 0$, and $\varepsilon_v \cdot \varepsilon_p = 0$. Based on the transmission direction in the transmitter coordinate system, we have

$$\varepsilon_p = [\sin \theta \cos \phi, \sin \theta \sin \phi, \cos \theta]^T, \quad (1)$$

where $\{\cdot\}^T$ is the transpose operation. The choice of ε_h and ε_v is not unique. Based on the orthogonality of these three unit vectors, normally we assume

$$\begin{aligned} \varepsilon_h &= [-\sin \phi, \cos \phi, 0]^T, \\ \varepsilon_v &= [\cos \theta \cos \phi, \cos \theta \sin \phi, -\sin \theta]^T. \end{aligned} \quad (2)$$

Here it can be seen that ε_h is parallel to the x-y plane, due to the zero value in the z direction, then ε_h is assumed as the unit vector of the horizontal component. Since ε_v is perpendicular to ε_p ($\varepsilon_v \cdot \varepsilon_p = 0$), ε_v is considered as the unit vector of the vertical component.

Moreover, we assume the electric field has transverse components [23], [24],

$$E = E_h \varepsilon_h + E_v \varepsilon_v, \quad (3)$$

where E_h and E_v correspond to the horizontal component and the vertical component, respectively [34], given by

$$\begin{bmatrix} E_h \\ E_v \end{bmatrix} = \begin{bmatrix} H e^{j\omega t} \\ V e^{j\omega t} \end{bmatrix} = \begin{bmatrix} a_h e^{j\psi_h} e^{j\omega t} \\ a_v e^{j\psi_v} e^{j\omega t} \end{bmatrix}, \quad (4)$$

where ω represents carrier frequency, H and V are complex numbers, a_h and a_v are amplitudes (positive and real-valued) of the horizontal and vertical components, and ψ_h and ψ_v are the corresponding initial phases. The polarisation ratio is represented by $\frac{V}{H} = \frac{a_v e^{j\psi_v}}{a_h e^{j\psi_h}} = (\tan \gamma) e^{j\eta}$ for $\gamma \in [0, \pi/2]$ and $\eta \in (-\pi, \pi]$, where $\tan \gamma$ represents the amplitude ratio, and η is the phase difference between two components [34]. Then the electric field can be given by

$$\begin{aligned} E &= E_h \varepsilon_h + E_v \varepsilon_v \\ &= A((\cos \gamma) \varepsilon_h + (\sin \gamma) e^{j\eta} \varepsilon_v) \\ &= A((- \cos \gamma \sin \phi + (\sin \gamma) e^{j\eta} \cos \theta \cos \phi) \hat{x} \\ &\quad + (\cos \gamma \cos \phi + (\sin \gamma) e^{j\eta} \cos \theta \sin \phi) \hat{y} \\ &\quad - ((\sin \gamma) e^{j\eta} \sin \theta) \hat{z}), \end{aligned} \quad (5)$$

where the amplitude A of the polarised signal is $A = \sqrt{|H|^2 + |V|^2}$, and the carrier wave $e^{j\omega t}$ is ignored. Considering the x- and y-axes where these dipoles are placed, the spatial-polarisation coherent vector \mathbf{s}_p [30], [35] can be given by

$$\begin{aligned} \mathbf{s}_p(\theta, \phi, \gamma, \eta) &= \begin{bmatrix} s_{px}(\theta, \phi, \gamma, \eta) \\ s_{py}(\theta, \phi, \gamma, \eta) \end{bmatrix} \\ &= \begin{bmatrix} -\cos \gamma \sin \phi + (\sin \gamma) e^{j\eta} \cos \theta \cos \phi \\ \cos \gamma \cos \phi + (\sin \gamma) e^{j\eta} \cos \theta \sin \phi \end{bmatrix}. \end{aligned} \quad (6)$$

The spatial steering vector of the array for transmission is a function of θ and ϕ , given by

$$\mathbf{s}_s(\theta, \phi) = [1, e^{-j\omega d_1 \sin \theta \sin \phi / c}, \dots, e^{-j\omega d_{N-1} \sin \theta \sin \phi / c}]^T, \quad (7)$$

where c is the speed of propagation. The steering vector of the array is the Kronecker product of spatial-polarisation coherent vector $\mathbf{s}_p(\theta, \phi, \gamma, \eta)$ and spatial steering vector $\mathbf{s}_s(\theta, \phi)$. Then, the steering vectors of the two sub-arrays can be given by

$$\begin{aligned} \mathbf{s}_x(\theta, \phi, \gamma, \eta) &= s_{px}(\theta, \phi, \gamma, \eta) \mathbf{s}_s(\theta, \phi), \\ \mathbf{s}_y(\theta, \phi, \gamma, \eta) &= s_{py}(\theta, \phi, \gamma, \eta) \mathbf{s}_s(\theta, \phi). \end{aligned} \quad (8)$$

The beam response of the array is [36]

$$p(\theta, \phi, \gamma, \eta) = \mathbf{w}^H \mathbf{s}(\theta, \phi, \gamma, \eta), \quad (9)$$

where $\{\cdot\}^H$ represents the Hermitian transpose, $\mathbf{s}(\theta, \phi, \gamma, \eta)$ is the $2N \times 1$ steering vector of the array

$$\begin{aligned} \mathbf{s}(\theta, \phi, \gamma, \eta) &= [\mathbf{s}_x(\theta, \phi, \gamma, \eta), \mathbf{s}_y(\theta, \phi, \gamma, \eta)]^T, \\ \mathbf{s}_x(\theta, \phi, \gamma, \eta) &= [s_{0,x}(\theta, \phi, \gamma, \eta), \dots, s_{N-1,x}(\theta, \phi, \gamma, \eta)]^T, \\ \mathbf{s}_y(\theta, \phi, \gamma, \eta) &= [s_{0,y}(\theta, \phi, \gamma, \eta), \dots, s_{N-1,y}(\theta, \phi, \gamma, \eta)]^T, \end{aligned} \quad (10)$$

and \mathbf{w} is the complex-valued weight vector

$$\mathbf{w} = [w_{0,x}, \dots, w_{N-1,x}, w_{0,y}, \dots, w_{N-1,y}]^T. \quad (11)$$

III. DIRECTIONAL MODULATION DESIGN

A. DESIGN WITH A FIXED CROSSED-DIPOLE ARRAY

In the current DM field, there is only one signal transmitted at one carrier frequency to the desired direction, and the weight coefficients are thus designed for one single signal. To increase channel capacity, in this section, we design a new DM scheme where a pair of orthogonally polarised signals can be transmitted at the same carrier frequency simultaneously without crossover. In detail, we need to find a set of weight coefficients for these two signals (s_1 and s_2). We use $\mathbf{s}(\theta, \phi, \gamma_1, \eta_1)$, $\mathbf{s}(\theta, \phi, \gamma_2, \eta_2)$, $p(\theta, \phi, \gamma_1, \eta_1)$, and $p(\theta, \phi, \gamma_2, \eta_2)$ to represent the steering vectors for s_1 and s_2 , and beam responses for s_1 and s_2 , respectively.

Here, we assume ϕ is fixed, and r points in the mainlobe and $R - r$ points in the sidelobe for both s_1 and s_2 are sampled. Then, we can construct a $2N \times 2r$ matrix \mathbf{S}_{ML} for steering vectors of two signals in the mainlobe, and a $2N \times 2(R - r)$ matrix \mathbf{S}_{SL} including all steering vectors over the sidelobe range [6],

$$\begin{aligned} \mathbf{S}_{SL} &= [\mathbf{s}(\theta_0, \phi, \gamma_1, \eta_1), \dots, \mathbf{s}(\theta_{R-r-1}, \phi, \gamma_1, \eta_1) \\ &\quad \mathbf{s}(\theta_0, \phi, \gamma_2, \eta_2), \dots, \mathbf{s}(\theta_{R-r-1}, \phi, \gamma_2, \eta_2)], \\ \mathbf{S}_{ML} &= [\mathbf{s}(\theta_{R-r}, \phi, \gamma_1, \eta_1), \dots, \mathbf{s}(\theta_{R-1}, \phi, \gamma_1, \eta_1) \\ &\quad \mathbf{s}(\theta_{R-r}, \phi, \gamma_2, \eta_2), \dots, \mathbf{s}(\theta_{R-1}, \phi, \gamma_2, \eta_2)]. \end{aligned} \quad (12)$$

Moreover, for M -ary signaling of modulation, each of s_1 and s_2 can create M constellation points (M symbols), leading to M desired responses. Since both signals are transmitted simultaneously, there are in total M^2 different symbols and M^2 sets of response pairs. According to the direction of the elevation angle θ , we define $\mathbf{p}_{SL,m}$ and $\mathbf{p}_{ML,m}$ as beam

responses over the sidelobe and mainlobe directions for the m -th combined symbol, where $m = 0, \dots, M^2 - 1$,

$$\begin{aligned} \mathbf{p}_{SL,m} &= [p_m(\theta_0, \phi, \gamma_1, \eta_1), \dots, p_m(\theta_{R-r-1}, \phi, \gamma_1, \eta_1) \\ &\quad p_m(\theta_0, \phi, \gamma_2, \eta_2), \dots, p_m(\theta_{R-r-1}, \phi, \gamma_2, \eta_2)], \\ \mathbf{p}_{ML,m} &= [p_m(\theta_{R-r}, \phi, \gamma_1, \eta_1), \dots, p_m(\theta_{R-1}, \phi, \gamma_1, \eta_1) \\ &\quad p_m(\theta_{R-r}, \phi, \gamma_2, \eta_2), \dots, p_m(\theta_{R-1}, \phi, \gamma_2, \eta_2)]. \end{aligned} \quad (13)$$

Then, the weight coefficients for the m -th combined symbol can be solved by

$$\begin{aligned} \min_{\mathbf{w}_m} \quad & \|\mathbf{p}_{SL,m} - \mathbf{w}_m^H \mathbf{S}_{SL}\|_2 \\ \text{subject to} \quad & \mathbf{w}_m^H \mathbf{S}_{ML} = \mathbf{p}_{ML,m}, \end{aligned} \quad (14)$$

where $\mathbf{w}_m = [w_{0,x,m}, \dots, w_{N-1,x,m}, w_{0,y,m}, \dots, w_{N-1,y,m}]^T$ corresponds to the m -th response pair $\mathbf{p}_m(\theta, \phi, \gamma, \eta) = [\mathbf{p}_{SL,m}, \mathbf{p}_{ML,m}]$, and $\|\cdot\|_2$ denotes the l_2 norm. The problem in (14) can be solved by the method of Lagrange multipliers and the optimum value for the coefficients \mathbf{w}_m can be found in our earlier conference publication [19], which is given by

$$\begin{aligned} \mathbf{w}_m &= \mathbf{R}^{-1} (\mathbf{S}_{SL} \mathbf{p}_{SL,m}^H - \mathbf{S}_{ML} ((\mathbf{S}_{ML}^H \mathbf{R}^{-1} \mathbf{S}_{ML})^{-1} \\ &\quad \times (\mathbf{S}_{ML}^H \mathbf{R}^{-1} \mathbf{S}_{SL} \mathbf{p}_{ML,m}^H - \mathbf{p}_{ML,m}))), \end{aligned} \quad (15)$$

with $\mathbf{R} = \mathbf{S}_{SL} \mathbf{S}_{SL}^H$.

B. SPARSE ARRAY DESIGN

Uniform linear arrays (ULAs) are widely used for DM; however, this is not the most effective way to achieve DM in terms of the number of antennas. To reduce the number of antennas but keep the antenna array performance, sparse arrays can be used in the context of DM [5], [6]. The idea of sparse array design using CS-based methods is to find the minimum number of non-zero valued weight coefficients from a large number of potential antennas to generate a response close to the desired one. As antennas with zero-valued coefficients are removed, the objective function for finding the minimum number of weight coefficients can be given by $\min \|\mathbf{w}\|_1$, where the l_1 norm $\|\cdot\|_1$ is used as an approximation to the l_0 norm $\|\cdot\|_0$. The constraint for keeping the difference between desired and designed responses under a given threshold value can be written as $\|\mathbf{p} - \mathbf{w}^H \mathbf{S}\|_2 \leq \alpha$, where α represents the allowed difference. Based on this idea of sparse array design, weight vector \mathbf{w}_m for the m -th set of constellation points in (14) can be adjusted to

$$\begin{aligned} \min_{\mathbf{w}_m} \quad & \|\mathbf{w}_m\|_1 \\ \text{subject to} \quad & \|\mathbf{p}_{SL,m} - \mathbf{w}_m^H \mathbf{S}_{SL}\|_2 \leq \alpha \\ & \mathbf{w}_m^H \mathbf{S}_{ML} = \mathbf{p}_{ML,m}. \end{aligned} \quad (16)$$

As the location optimisation in (16) is calculated individually for each set of constellation points, a common set of active crossed-dipole positions cannot be guaranteed for all symbol pairs; in other words, the antenna with weight coefficients which are zero-valued for some symbols but non-zero-valued for others, cannot be removed. To solve the

problem, group sparsity is introduced [33] to find a common set of active antenna locations for all sets of constellation points. Therefore, we introduce $\tilde{\mathbf{w}}_n$ to allow all elements in the vector to be minimised simultaneously, e.g. to remove the n -th antenna, the vector $\tilde{\mathbf{w}}_n$ needs to be zero-valued

$$\tilde{\mathbf{w}}_n = [w_{n,x,0}, \dots, w_{n,x,M^2-1}, w_{n,y,0}, \dots, w_{n,y,M^2-1}]. \quad (17)$$

Then, the cost function for finding the minimum number of antenna locations can be considered as finding $\min \|\hat{\mathbf{w}}\|_1$, where $\hat{\mathbf{w}}$ gathers all $\|\tilde{\mathbf{w}}_n\|_2$ for $n = 0, \dots, N - 1$,

$$\hat{\mathbf{w}} = [\|\tilde{\mathbf{w}}_0\|_2, \|\tilde{\mathbf{w}}_1\|_2, \dots, \|\tilde{\mathbf{w}}_{N-1}\|_2]^T. \quad (18)$$

Moreover, to impose DM constraints on all constellation points, the following matrices are constructed

$$\mathbf{W} = [\mathbf{w}_0, \mathbf{w}_1, \dots, \mathbf{w}_{M^2-1}], \quad (19)$$

$$\mathbf{P}_{SL} = [\mathbf{p}_{SL,0}, \mathbf{p}_{SL,1}, \dots, \mathbf{p}_{SL,M^2-1}]^T, \quad (20)$$

$$\mathbf{P}_{ML} = [\mathbf{p}_{ML,0}, \mathbf{p}_{ML,1}, \dots, \mathbf{p}_{ML,M^2-1}]^T. \quad (21)$$

As the reweighted l_1 norm minimisation has a closer approximation to the l_0 norm [37]–[39], the corresponding iteration based formulations for sparse array design becomes

$$\begin{aligned} \min_{\mathbf{W}} \quad & \sum_{n=0}^{N-1} \delta_n^u \|\tilde{\mathbf{w}}_n^u\|_2 \\ \text{subject to} \quad & \|\mathbf{P}_{SL} - (\mathbf{W}^u)^H \mathbf{S}_{SL}\|_2 \leq \alpha \\ & (\mathbf{W}^u)^H \mathbf{S}_{ML} = \mathbf{P}_{ML}, \end{aligned} \quad (22)$$

where the superscript u indicates the u -th iteration, and δ_n is the reweighting term for the n -th row of coefficients, given by $\delta_n^u = (\|\tilde{\mathbf{w}}_n^{u-1}\|_2 + \xi)^{-1}$. The above problem can be solved using *cvx*, a package for specifying and solving convex problems [40], [41].

To receive and separate two orthogonally polarised signals, a crossed-dipole antenna or array is needed [30], and polarisations of the antennas at the receiver side in the desired direction do not need to match those of the transmitted signals, as cross-interference due to polarisation mismatch can be suppressed using standard signal processing techniques such as the Wiener filter when a reference signal is available [20].

IV. DESIGN EXAMPLES

In this section, design examples are provided to show the performance of the proposed design methods for both ULAs and sparse antenna arrays. For each of s_1 and s_2 , the desired response is a value of one (magnitude) with a given phase at the mainlobe (QPSK), i.e., symbols ‘00’, ‘01’, ‘11’, ‘10’ correspond to 45° , 135° , -45° and -135° , respectively, and a value of 0.1 (magnitude) with random phase over the sidelobe regions. Therefore, for signals s_1 and s_2 transmitted simultaneously, we can construct 16 different combined symbols. The polarisation states for s_1 are defined by $(\gamma_1, \eta_1) = (0^\circ, 0^\circ)$ for a horizontal polarisation, and $(\gamma_2, \eta_2) = (90^\circ, 0^\circ)$ for s_2 for a vertical polarisation. Moreover, both broadside and off-broadside designs are studied.

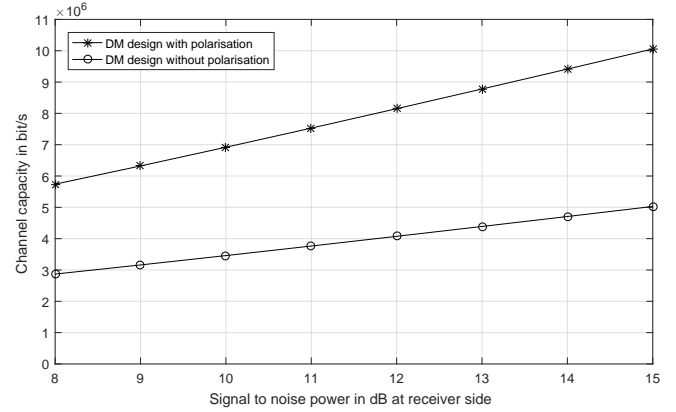


FIGURE 2: Channel capacity verse SNR at the desired location.

For broadside design, the mainlobe direction is assumed to be $\theta_{ML} = 0^\circ$ for $\phi = 90^\circ$ and the sidelobe regions are $\theta_{SL} \in [5^\circ, 90^\circ]$ for $\phi = \pm 90^\circ$. For the off-broadside design, the desired direction is $\theta_{ML} = 30^\circ$ for $\phi = 90^\circ$, while the sidelobe regions are $\theta_{SL} \in \{[0, 25^\circ], [35^\circ, 90^\circ]\}$ for $\phi = 90^\circ$, and $\theta_{SL} \in [0, 90^\circ]$ for $\phi = -90^\circ$, sampled every 1° .

For sparse antenna array design, to have a fair comparison, we first obtain the DM result by (14) based on a 9λ aperture ULA with a half wavelength spacing between adjacent antennas. Then we set the error norm between the desired and designed responses from (14) as the allowed difference α in (22) for sparse array designs.

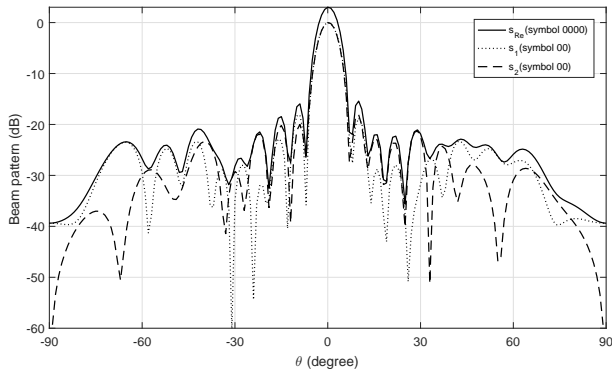
To verify the performance of each design, the corresponding beam and phase patterns are given. Moreover, bit error rate (BER) is calculated based on in which quadrant the received point lies in the complex plane. Here the signal to noise ratio (SNR) is set at 12 dB in the mainlobe direction, then with the average power (1) of all randomly generated 10^6 transmitted bits in the mainlobe, the noise variance σ^2 is 0.0631. Assuming the additive white Gaussian noise (AWGN) level is the same for all directions, then a random noise with this power level can be generated for each direction.

A. ADVANTAGE OF THE POLARISATION DESIGN OVER UN-POLARISATION'S

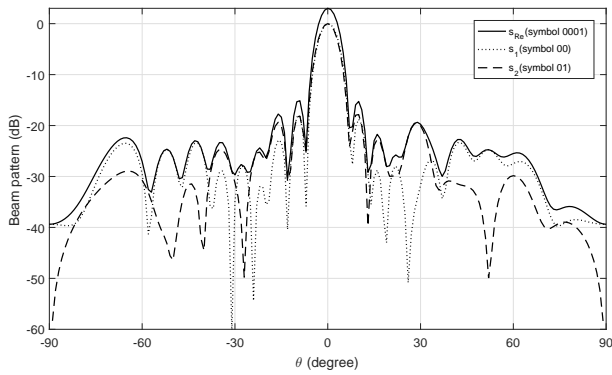
Fig 2 shows the channel capacity verse SNR. Here the bandwidth of the channel is set to 1MHz, then we can see that with an increased SNR, channel capacity grow for both designs, and the channel capacity for polarisation design is two times more than non-polarisation's.

B. BROADSIDE EXAMPLES OF POLARISATION DESIGN

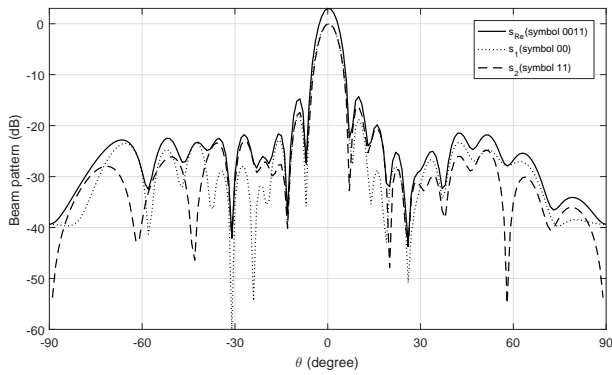
Based on the given antenna array design in (14), Fig. 3 shows the beam responses for symbols ‘00,00’, ‘00,01’, ‘00,11’ and ‘00,10’. It can be observed that all main beams are exactly pointed to 0° (the desired direction) with a low sidelobe level. The mainlobe power level for the composite signal



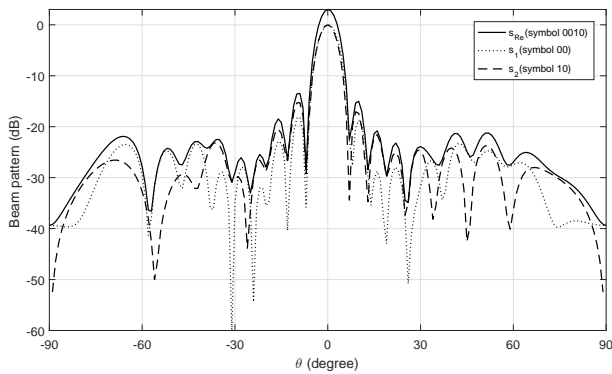
(a)



(b)

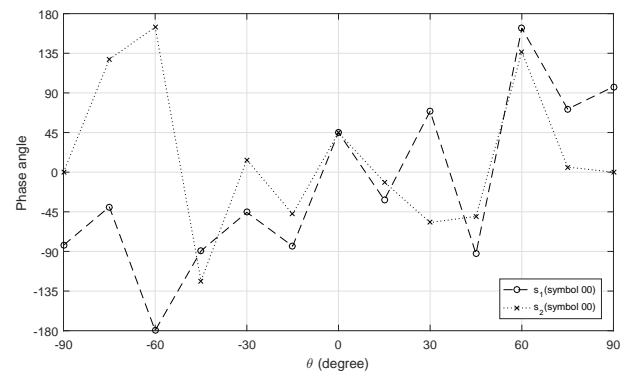


(c)

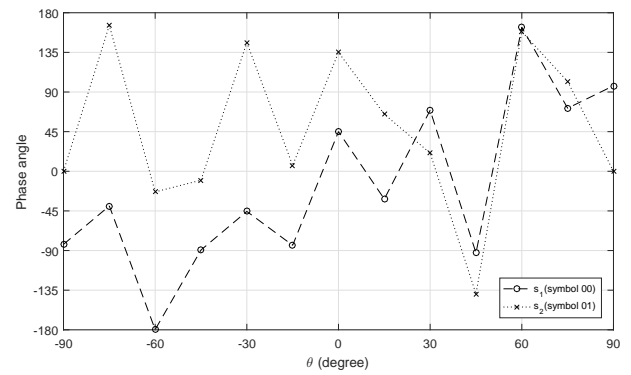


(d)

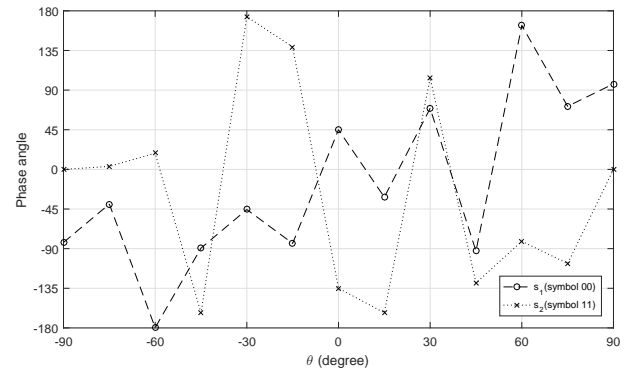
FIGURE 3: Resultant beam responses based on the broad-side ULA design (14) for symbols (a) ‘00,00’, (b) ‘00,01’, (c) ‘00,11’, (d) ‘00,10’.



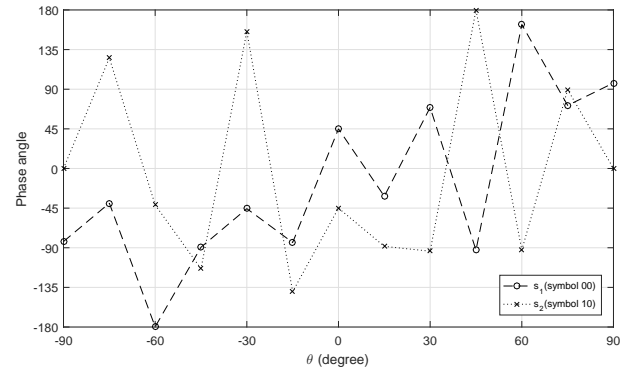
(a)



(b)

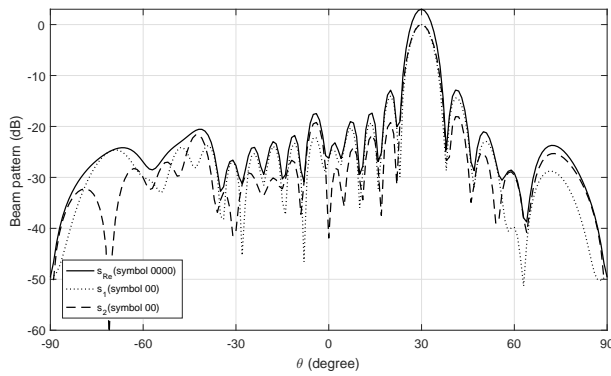


(c)

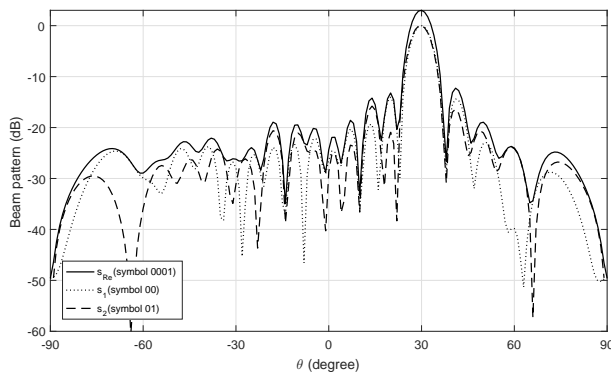


(d)

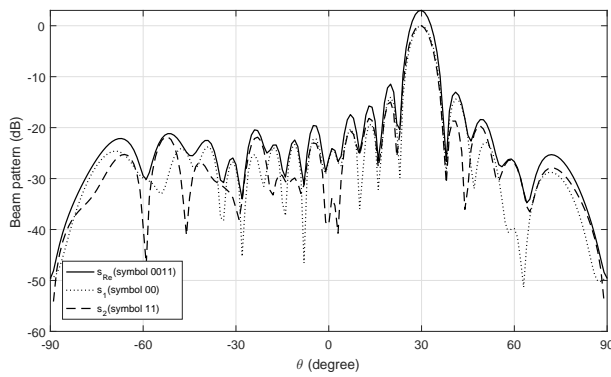
FIGURE 4: Resultant phase responses based on the broad-side ULA design (14) for symbols (a) ‘00,00’, (b) ‘00,01’, (c) ‘00,11’, (d) ‘00,10’.



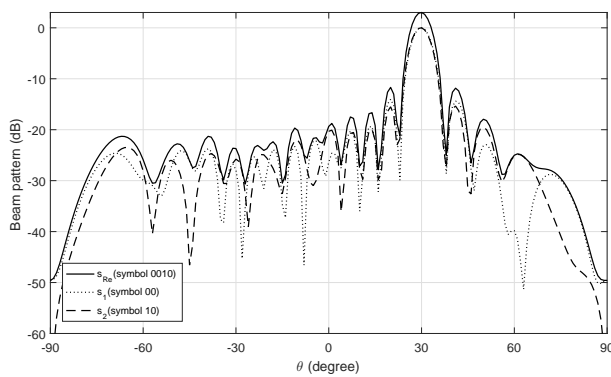
(a)



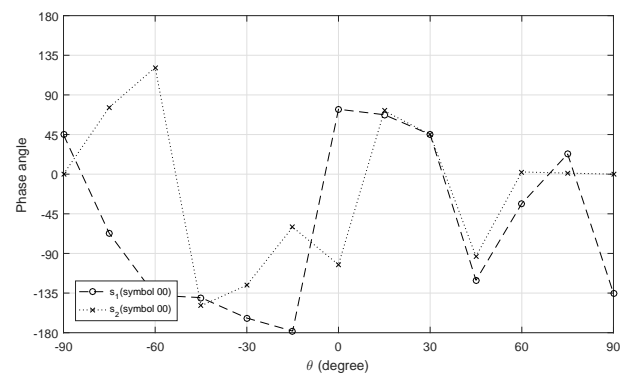
(b)



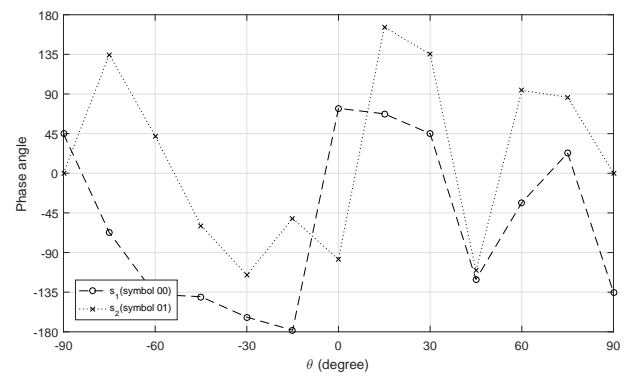
(c)



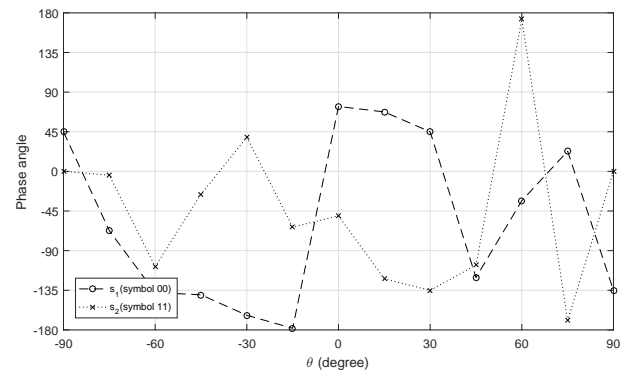
(d)



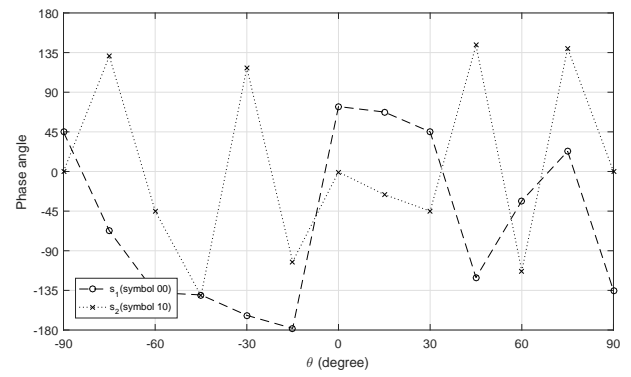
(a)



(b)



(c)



(d)

FIGURE 5: Resultant beam responses based on the off-broadside ULA design (14) for symbols (a) ‘00,00’, (b) ‘00,01’, (c) ‘00,11’, (d) ‘00,10’.

FIGURE 6: Resultant phase responses based on the off-broadside ULA design (14) for symbols (a) ‘00,00’, (b) ‘00,01’, (c) ‘00,11’, (d) ‘00,10’.

$s_{Re} = s_1 + s_2j$ is 3.01dB ($\sqrt{2}$ magnitude), and its corresponding components for s_1 and s_2 coincide in the mainlobe direction with 0dB power level. The phases of s_1 and s_2 are shown Fig. 4, where in the desired direction the phases are in accordance with the standard QPSK constellation, while phases are random for the rest of the angles. The beam and phase patterns for other symbols are not shown as they have the same features as the aforementioned figures.

Based on the value of error norm α from the above ULA design result, the maximum aperture of the designed crossed-dipole array is set to be 20λ with 201 equally spaced potential antennas. Moreover, $\xi = 0.001$ indicates the threshold for active antennas.

For the reweighted l_1 norm minimisation method in (22), the number of active antennas is 14, with an average spacing of 0.9231λ , where the antenna locations are given in Table 1. The beam and phase patterns for these 16 combined symbols are similar to the ULA design, all indicating a satisfactory DM design result.

C. OFF-BROADSIDE EXAMPLES OF POLARISATION DESIGN

Figs. 5 and 6 show the beam and phase responses for the corresponding symbols ‘00,00’, ‘00,01’, ‘00,11’ and ‘00,10’ based on the ULA design, respectively. It can be seen that all main beams are exactly pointed to 30° (the desired direction) with a low sidelobe level, and phases in this direction follow QPSK modulation pattern with scrambled values in other directions. The beam and phase patterns for other symbols have the same features as the aforementioned figures. The sparse array designs produce similar patterns to the ULA design, and the optimised locations are shown in Table 3, with the performance results in Table 4.

D. BER FOR BROADSIDE AND OFF-BROADSIDE DESIGNS

BER can be represented by the following equation

$$BER = \frac{\text{Error bits}}{\text{Total number of bits}}. \quad (23)$$

Fig. 7 shows the BER performance based on broadside and off-broadside ULA designs. Sparse array designs have a similar result. Here we can see that for both designs the achieved BER is down to 10^{-5} in desired directions, while at other directions it fluctuates around 0.5.

Note that some BER values are higher than 0.5, which is possible, because in the design, even without having any noise at the receiver side, there is already a phase bias in the received signal, resulted from scrambled phases setting for pattern synthesis, due to the DM design. For example, assume we want to send the symbol 00 using the constellation point (1, 1) in the desired direction, and the resultant constellation coordinates in another direction could be $(-0.3, -0.4)$, which ends up representing ‘11’, with complete error for these two bits.

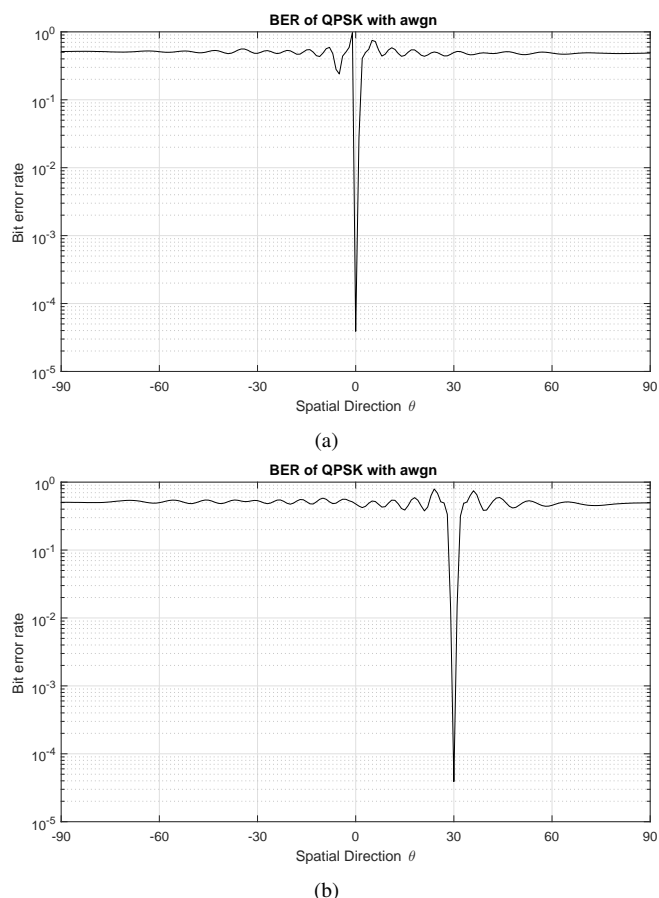


FIGURE 7: BER performance: (a) broadside ULA design, (b) off-broadside ULA design.

TABLE 1: Optimised antenna locations based on the reweighted l_1 norm minimisation for broadside design.

n	d_n/λ	n	d_n/λ	n	d_n/λ
0	0	5	4.7	10	9.2
1	1	6	5.6	11	10.2
2	1.9	7	6.5	12	11.1
3	2.8	8	7.4	13	12
4	3.7	9	8.3		

TABLE 2: Summary of the broadside design results.

	ULA	Reweighted l_1
Antenna number	19	14
Aperture/ λ	9	12
Average spacing/ λ	0.5	0.9231
$\ P_{SL} - W^H S_{SL}\ _2$	7.9968	7.8547

TABLE 3: Optimised antenna locations based on the reweighted l_1 norm minimisation for off-broadside design.

n	d_n/λ	n	d_n/λ	n	d_n/λ
0	0	6	5	12	8.4
1	1.3	7	5.8	13	9
2	1.8	8	6.3	14	9.5
3	3.2	9	6.9	15	10.3
4	3.7	10	7.5	16	10.6
5	4.6	11	7.9	17	11.3

TABLE 4: Summary of the off-broadside design results.

	ULA	Reweighted l_1
Antenna number	19	18
Aperture/ λ	9	11.3
Average spacing/ λ	0.5	0.6647
$\ P_{SL} - W^H S_{SL}\ _2$	8.7887	8.7875

V. CONCLUSIONS

A crossed-dipole antenna array for directional modulation is proposed, and array designs for two signals s_1 and s_2 with orthogonal polarisation states transmitted to the same direction at the same frequency are studied. The channel capacity based on the polarisation design doubles the capacity for the case where polarisation information is not considered, which is the main advantage resulted from the proposed scheme. The proposed design is first applied to a given antenna array geometry, and a closed-form solution is provided. Then, the proposed design is introduced to sparse arrays for finding optimised antenna locations via the reweighted l_1 norm minimisation method. As shown in the provided design examples, the resultant main beams can point to the desired direction (either broadside or off-broadside) with desired phase pattern, while a low sidelobe level and scrambled phases are formed in other directions.

REFERENCES

- [1] A. Babakhani, D. B. Rutledge, and A. Hajimiri. Transmitter architectures based on near-field direct antenna modulation. *IEEE Journal of Solid-State Circuits*, 43(12):2674–2692, December 2008.
- [2] A. Babakhani, D. B. Rutledge, and A. Hajimiri. Near-field direct antenna modulation. *IEEE Microwave Magazine*, 10(1):36–46, February 2009.
- [3] M. P. Daly and J. T. Bernhard. Beamsteering in pattern reconfigurable arrays using directional modulation. *IEEE Transactions on Antennas and Propagation*, 58(7):2259–2265, March 2010.
- [4] M. P. Daly and J. T. Bernhard. Directional modulation technique for phased arrays. *IEEE Transactions on Antennas and Propagation*, 57(9):2633–2640, September 2009.
- [5] B. Zhang, W. Liu, and X. Gou. Compressive sensing based sparse antenna array design for directional modulation. *IET Microwaves, Antennas Propagation*, 11(5):634–641, April 2017.
- [6] B. Zhang and W. Liu. Multi-carrier based phased antenna array design for directional modulation. *IET Microwaves, Antennas Propagation*, 12(5):765–772, April 2018.
- [7] J. Hu, S. Yan, F. Shu, J. Wang, J. Li, and Y. Zhang. Artificial-noise-aided secure transmission with directional modulation based on random frequency diverse arrays. *IEEE Access*, 5:1658–1667, 2017.
- [8] F. Shu, L. Xu, J. Wang, W. Zhu, and Z. Xiaobo. Artificial-noise-aided secure multicast precoding for directional modulation systems. *IEEE Transactions on Vehicular Technology*, 67(7):6658–6662, July 2018.
- [9] F. Shu, X. Wu, J. Hu, J. Li, R. Chen, and J. Wang. Secure and precise wireless transmission for random-subcarrier-selection-based directional modulation transmit antenna array. *IEEE Journal on Selected Areas in Communications*, 36(4):890–904, April 2018.
- [10] F. Shu, Y. Qin, T. Liu, L. Gui, Y. Zhang, J. Li, and Z. Han. Low-complexity and high-resolution doa estimation for hybrid analog and digital massive mimo receive array. *IEEE Transactions on Communications*, 66(6):2487–2501, June 2018.
- [11] T. Hong, M. Z. Song, and Y. Liu. Dual-beam directional modulation technique for physical-layer secure communication. *IEEE Antennas and Wireless Propagation Letters*, 10:1417–1420, December 2011.
- [12] H. Z. Shi and A. Tennant. Enhancing the security of communication via directly modulated antenna arrays. *IET Microwaves, Antennas & Propagation*, 7(8):606–611, June 2013.
- [13] Y. Ding and V. Fusco. Directional modulation transmitter radiation pattern considerations. *IET Microwaves, Antennas & Propagation*, 7(15):1201–1206, December 2013.
- [14] T. Xie, J. Zhu, and Y. Li. Artificial-noise-aided zero-forcing synthesis approach for secure multi-beam directional modulation. *IEEE Communications Letters*, PP(99):1–1, 2017.
- [15] W. Zhu, F. Shu, T. Liu, X. Zhou, J. Hu, G. Liu, L. Gui, J. Li, and J. Lu. Secure precise transmission with multi-relay-aided directional modulation. In *2017 9th International Conference on Wireless Communications and Signal Processing (WCSP)*, pages 1–5, October 2017.
- [16] B. Guo, Y. Yang, G. Xin, and Y. Tang. Combinatorial interference directional modulation for physical layer security transmission. In *2016 IEEE Information Technology, Networking, Electronic and Automation Control Conference*, pages 710–713, May 2016.
- [17] M. Hafez, T. Khattab, T. Elfouly, and H. Arslan. Secure multiple-users transmission using multi-path directional modulation. In *2016 IEEE International Conference on Communications (ICC)*, pages 1–5, May 2016.
- [18] B. Zhang and W. Liu. Antenna array based positional modulation with a two-ray multi-path model. In *Proc. Sensor Array and Multichannel signal processing workshop 2018 (SAM2018)*, Sheffield, UK, July 2018, to appear.
- [19] B. Zhang, W. Liu, and X. Lan. Directional modulation design based on crossed-dipole arrays for two signals with orthogonal polarisations. In *Proc. European Conference on Antennas and Propagation (EuCAP)*, London, UK, April 2018.
- [20] W. Liu. Channel equalization and beamforming for quaternion-valued wireless communication systems. *Journal of the Franklin Institute*, 354(18):8721 – 8733, 2017.
- [21] O. M. Isaeva and V. A. Sarytchev. Quaternion presentations polarization state. In *Proc. 2nd IEEE Topical Symposium of Combined Optical-Microwave Earth and Atmosphere Sensing*, pages 195–196, Atlanta, US, April 1995.
- [22] L. H. Zetterberg and H. Brandstrom. Codes for combined phase and amplitude modulated signals in a four-dimensional space. *IEEE Transactions on Communications*, 25(29):943–950, September 1977.
- [23] R. T. Compton. On the performance of a polarization sensitive adaptive array. *IEEE Transactions on Antennas and Propagation*, 29(5):718–725, September 1981.
- [24] R. T. Compton. The tripole antenna: An adaptive array with full polarization flexibility. *IEEE Transactions on Antennas and Propagation*, 29(6):944–952, November 1981.
- [25] A. Nehorai and E. Paldi. *Digital Signal Processing Handbook*, chapter Electromagnetic vector-sensor array processing, pages 65.1–65.26. CRC Press, 1998.
- [26] S. Miron, N. Le Bihan, and J. I. Mars. Quaternion-MUSIC for vector-sensor array processing. *IEEE Transactions on Signal Processing*, 54(4):1218–1229, April 2006.
- [27] X. M. Gou, Y. G. Xu, Z. W. Liu, and X. F. Gong. Quaternion-Capon beamformer using crossed-dipole arrays. In *Proc. IEEE International Symposium on Microwave, Antenna, Propagation, and EMC Technologies for Wireless Communications (MAPE)*, pages 34–37, Beijing, China, November 2011.
- [28] M. B. Hawes and W. Liu. Design of fixed beamformers based on vector-sensor arrays. *International Journal of Antennas and Propagation*, 2015:181937.1–181937.9, March 2015.
- [29] J. J. Xiao and A. Nehorai. Optimal polarized beampattern synthesis using a vector antenna array. *IEEE Transactions on Signal Processing*, 57(2):576–587, February 2009.
- [30] X. Lan and W. Liu. Fully quaternion-valued adaptive beamforming based on crossed-dipole arrays. *Electronics*, 6(2):34, April 2017.
- [31] A. Moffet. Minimum-redundancy linear arrays. *IEEE Transactions on Antennas and Propagation*, 16(2):172–175, March 1968.
- [32] H. L. Van Trees. *Optimum Array Processing, Part IV of Detection, Estimation, and Modulation Theory*. Wiley, New York, 2002.
- [33] Q. Shen, W. Liu, W. Cui, S. L. Wu, Y. D. Zhang, and M. Amin. Low-complexity direction-of-arrival estimation based on wideband co-prime arrays. *IEEE Trans. Audio, Speech and Language Processing*, 23(9):1445–1456, September 2015.
- [34] G. A. Deschamps. Techniques for handling elliptically polarized waves with special reference to antennas: Part II - geometrical representation of the polarization of a plane electromagnetic wave. *Proceedings of the IRE*, 39(5):540–544, May 1951.
- [35] X. R. Zhang, W. Liu, Y. G. Xu, and Z. W. Liu. Quaternion-valued robust adaptive beamformer for electromagnetic vector-sensor arrays with worst-case constraint. *Signal Processing*, 104:274–283, April 2014.

- [36] M. B. Hawes, W. Liu, and L. Mihaylova. Compressive sensing based design of sparse tripole arrays. *Sensors*, 15(12):31056–31068, December 2015.
- [37] E. J. Candès, M. B. Wakin, and S. P. Boyd. Enhancing sparsity by reweighted l_1 minimization. *Journal of Fourier Analysis and Applications*, 14(5):877–905, 2008.
- [38] G. Prisco and M. D’Urso. Maximally sparse arrays via sequential convex optimizations. *IEEE Antennas and Wireless Propagation Letters*, 11:192–195, February 2012.
- [39] B. Fuchs. Synthesis of sparse arrays with focused or shaped beam pattern via sequential convex optimizations. *IEEE Transactions on Antennas and Propagation*, 60(7):3499–3503, May 2012.
- [40] M. Grant and S. Boyd. Graph implementations for nonsmooth convex programs. In V. Blondel, S. Boyd, and H. Kimura, editors, *Recent Advances in Learning and Control*, Lecture Notes in Control and Information Sciences, pages 95–110. Springer-Verlag Limited, 2008. [http://stanford.edu/~boyd/graph/\\$_sdc.html](http://stanford.edu/~boyd/graph/$_sdc.html).
- [41] CVX Research. CVX: Matlab software for disciplined convex programming, version 2.0 beta. <http://cvxr.com/cvx>, September 2012.



XIANG LAN received his Bsc from Huazhong University of Science and Technology, China, in 2012. He received his Msc in 2014 and is working for his PhD in the Department of Electrical and Electronic Engineering, University of Sheffield. His research interests cover signal processing based on vector sensor array (beamforming and DOA estimation with polarized signals) and sparse array processing.

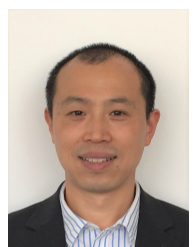
...



BO ZHANG received his BSc from Tianjin Normal University, China, in 2011. MSc and PhD from the Department of Electrical and Electronic Engineering, University of Sheffield in 2013 and 2018, respectively.

He is working with the College of Electronic and Communication Engineering, Tianjin Normal University. His research interests cover array signal processing (beamforming and direction of arrival estimation, etc.), directional modulation and

sparse array design.



WEI LIU (S’01-M’04-SM’10) received his BSc and LLB. degrees from Peking University, China, in 1996 and 1997, respectively, MPhil from the University of Hong Kong in 2001, and PhD from the School of Electronics and Computer Science, University of Southampton, UK, in 2003. He then worked as a postdoc first at Southampton and later at the Department of Electrical and Electronic Engineering, Imperial College London.

Since September 2005, he has been with the Department of Electronic and Electrical Engineering, University of Sheffield, UK, first as a Lecturer and then a Senior Lecturer. He has published more than 250 journal and conference papers, three book chapters, and a research monograph about wideband beamforming "Wideband Beamforming: Concepts and Techniques" (John Wiley, March 2010). Another book titled "Low-Cost Smart Antennas" (by Wiley-IEEE) will appear in March 2019. His research interests cover a wide range of topics in signal processing, with a focus on sensor array signal processing (beamforming and source separation/extraction, direction of arrival estimation, target tracking and localisation, etc.), and its various applications, such as robotics and autonomous vehicles, human computer interface, big data analytics, radar, sonar, satellite navigation, and wireless communications.

He is a member of the Digital Signal Processing Technical Committee of the IEEE Circuits and Systems Society and the Sensor Array and Multichannel Signal Processing Technical Committee of the IEEE Signal Processing Society (Vice-Chair from Jan 2019). He is currently an Associate Editor for IEEE Trans. on Signal Processing and IEEE Access, and an editorial board member of the Journal Frontiers of Information Technology and Electronic Engineering.